Available online at www.sciencedirect.com
SCIENCE DIRECT®
Journal of Nuclear Materials 334 (2004) 149–158
journal of nuclear materials
www.elsevier.com/locate/jnucmat

Iodine transmutation studies using metal iodide targets

E. Ichimura [a], N. Takaki [b], R.P.C. Schram [c,*], R. Klein Meulekamp [c], K. Bakker [c]

[a] *Tokyo Electric Power Company (TEPCO), 4-1, Egasaki-cho, Tsurumi-ku, Yokohama, Japan*
[b] *TEPCO, Japan Nuclear Cycle Development Institute (JNC), 4002 Narita-cho, O-arai-machi, Higashi-ibaraki-gun, Ibaraki 311-1393, Japan*
[c] *Nuclear Research and Consultancy Group (NRG), P.O. Box 25, 1755 ZG Petten, The Netherlands*

Received 23 September 2003; accepted 14 May 2004

Abstract

This paper describes the preparation, irradiation and the post-irradiation examination of the Project-I iodine transmutation irradiation experiment. Capsules containing pellets of MgI_2, CaI_2, CuI and NaI have been irradiated in the High Flux Reactor (HFR) in Petten for 271.23 full power days. The post-irradiation examination includes neutron metrology, gamma spectrometry, chemical analysis, gas puncturing, gas analysis, metallography and EPMA.

1. Introduction

Iodine-129 presents a major contribution to the radiological risk of the spent fuel waste in the long term. Transmutation of ^{129}I to stable ^{130}Xe is therefore a means to reduce the radiological risk. It is necessary to find a proper chemical form for irradiation in which iodine is contained. Elemental iodine itself is a very volatile and corrosive compound and therefore not compatible with the currently used steel capsule materials. Alternative stable chemical forms such as metal iodide salts were therefore considered as transmutation targets. In the EFTTRA-T1 irradiation [1], three metal iodides were irradiated in the HFR: NaI, PbI_2 and CeI_3. NaI gave the best results from these three metal iodides, although NaI has the disadvantage of having the lowest iodine density of these three compounds. PbI_2 caused a strong corrosion, while CeI_3 appeared to be very sensitive to air and moisture. CeI_3 has the advantage of a low vapour pressure. Comparing the results on NaI, PbI_2 and CeI_3 lead to the conclusion that from these three candidate materials NaI was most suitable.

Since several other metal iodides exist that may have better properties than NaI [2,3] the present irradiation experiment is performed with the four metal iodides CuI, CaI_2, MgI_2 and NaI. An overview of the main properties of these iodides is shown in Table 1. These compounds were irradiated as pellets, whereas powders were used for the EFTTRA-T1 experiment. The reason for using pellets is that they were easier to handle and higher iodine densities can be obtained. One of the capsules containing NaI is equipped with a pressure transducer, such that the transmutation of ^{127}I to ^{128}Xe can be monitored on-line. The irradiation duration was 11 HFR cycles (271.23 full power days).

For the present irradiation test, only natural iodine (^{127}I) containing material has been used. Iodine originating from reprocessed LWR fuel contains about 16% ^{127}I and 84% ^{129}I [9]. The transmutation schemes of ^{127}I and ^{129}I are rather similar (Fig. 1), but some differences

* Corresponding author. Tel.: +31-224 564 362; fax: +31-224 568 608.
E-mail address: schram@nrg-nl.com (R.P.C. Schram).

0022-3115/$ - see front matter © 2004 Elsevier B.V. All rights reserved.
doi:10.1016/j.jnucmat.2004.05.012

Table 1
Properties of the selected iodides

	CaI_2	NaI	MgI_2	CuI
Thermal cross-section metal atom (barn)	0.43	0.54	0.064	3.79
Log(vapour pressure/bar) at $T = 575$ °C	−8.0	−4.7	−3.2	−3.9
Melting temperature (°C)	783 [5]	661 [4]	633 [5]	595 [6]
Melting temperature of metal (°C)	839	98	649	1085
Iodine density 100% dense mat. (g/cm^3)	3.46	3.10	4.04	3.75
Volume thermal expansion in specified temperature range		11.1% [8] (30–655 °C)		6.4% [7] (20–550 °C)

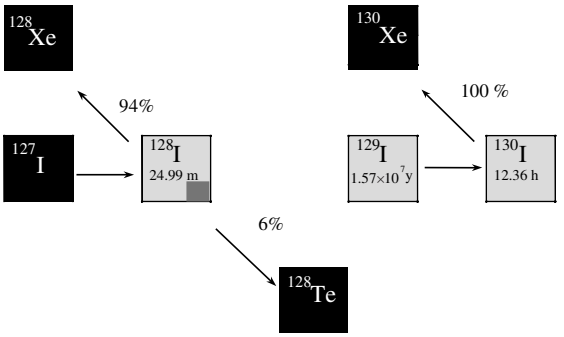

Fig. 1. The transmutation schemes of ^{127}I and ^{129}I.

can be identified. The resonance integral for ^{127}I is five times higher than that of ^{129}I, contrary to the thermal cross-section, which is five times lower. This rough comparison indicates that neutrons in the resonance region dominate the transmutation of ^{127}I, whereas the transmutation of ^{129}I is dominated by thermal neutrons. Another difference is the decay of ^{128}I and ^{130}I. The ^{128}I nuclide decays for 94% to ^{128}Xe, while 6% decay into the chalcogen tellurium. Chemical interaction experiments performed in the metal iodide selection process have shown that tellurium chemically interacts with the steel of the cladding. In the gas puncture analysis (Section 5.2) only the amount of xenon released is measured, from which the iodine transmutation extent can be estimated.

2. Irradiation targets

Five capsules containing four different metal iodide samples were irradiated, as shown in Table 2. The metal iodides contain natural iodine (^{127}I) and were obtained commercially. The metal iodides contained in the capsules were pressed pellets. Prior to pressing, the NaI and CaI_2 powder was dried at 400 °C in an argon atmosphere. The MgI_2 and CuI powder was not dried before pressing, because X-ray diffraction indicated that the as-received samples were already dry. Prior to irradiation, the powders of CuI, CaI_2, MgI_2 and NaI were characterised by chemical analysis and X-ray diffraction (XRD). All samples were phase pure (as determined by XRD), and the impurities as measured by ICP-AES were 0.16 wt% for CaI_2, and below 0.05 wt% for the other metal iodides. The metal iodides were pressed into pellets in a 5 mm diameter pressing dye at a pressing force of 250 MPa, except CuI which was pressed at 400 MPa. The higher pressing force was necessary to obtain integral CuI pellets. Data on the obtained pellets are shown in Table 2. The typical height of the pellets is 5 mm and all pellet stacks contain seven pellets. All the metal iodides were stored, handled and pressed in a glove box containing purified argon.

All capsules were made of AISI 316L steel tubes, with an inner diameter of 5.33 mm and an outer diameter of 6.35 mm. The typical pellet diameter is 5.03 mm, causing the gap between the pellets and the cladding to be about 150 μm. This gap can accommodate a volume expansion of about 9%, assuming isotropic expansion. Values for

Table 2
The test matrix of the project I irradiation

Capsule no.	Sample	Sample mass (g)	Stack height (mm)	Pellet diameter (mm)	Geometrical density		Iodine density (g/cm^3)
					(g/cm^3)	(%T.D.)	
6	MgI_2	2.92	34.2	5.026	4.30	97.0	3.92
7	CaI_2	2.61	35.4	5.034	3.70	92.3	3.19
8	CuI	3.59	35.9	5.027	5.04	89.7	3.36
9	NaI	2.43	36.2	5.023	3.39	92.4	2.86
10	NaI + PT[a]	2.42	36.0	5.023	3.40	92.7	2.87

[a] PT is pressure transducer.

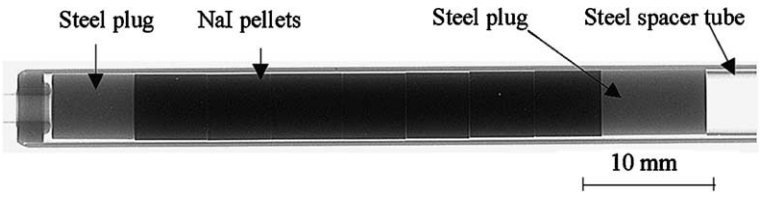

Fig. 2. X-ray image of capsule no. 10 (NaI) before irradiation.

the thermal expansion of the metal iodides are tabulated in Table 1, which show that the gap can more or less accommodate thermal expansion in the relevant temperature range without inducing mechanical stress on the cladding. The large thermal volume expansion is partially due to volume change associated with the high temperature change in crystal structure from face centre cubic to orthorhombic.

The height of each capsule is 310.5 mm. A hollow steel spacer tube keeps the pellets in their position. The filling gas of the capsules is helium (slightly more than 1 bar at room temperature). A large gas volume is present to accommodate the Xe pressure that builds up during the transmutation process. This gas volume (about 5 cm^3) is approximately seven times larger than the volume of the metal iodide stack (about 0.7 cm^3). One of the NaI containing capsules (capsule no. 10) was equipped with a pressure transducer for online monitoring of the total pressure. An X-ray image of the lower part of a representative capsule (capsule no. 10) is shown in Fig. 2.

3. Irradiation

The irradiation was performed in the High Flux Reactor in Petten at irradiation position C7. The duration of the irradiation was 11 cycles in the HFR, which is equivalent to a total irradiation time of 271.23 full power days. The cycle-to-cycle variation of the neutron flux conditions is less than 10%. During irradiation the capsules were placed in an aluminium drum in the sample holder. The instrumentation consists of 22 type K thermocouples, one pressure transducer, seven neutron fluence detector sets and five gamma-scan wires. The pressure transducer of capsule no. 10 failed at the end of the first irradiation cycle and therefore no pressure data have been included in the present paper. Another experiment with pressure transducer equipped NaI containing capsules was recently successfully completed, the results are to be published [8]. Each capsule is surrounded by at least three thermocouples placed at different axial positions, in order to determine both the aluminium temperature close to the metal iodide in the capsule and the aluminium temperature close to the gas-filled plenum of the capsules. Close to the metal iodide stack of each capsule a neutron fluence detector set is placed. Over the full length of the aluminium drum five gamma-scan wires were positioned close to each of the five capsules. Gamma-scan wire measurements after irradiation show that the neutron flux variation is smaller than 2% over the height of the metal iodide stack.

4. Neutronics

Neutronic simulations were carried out to determine the transmutation efficiency of the capsules and special attention was given to the influence of nuclear data and the effect of (self)shielding. To reduce the computational effort of this transmutation analysis use was made of two-step strategy in which the flux experienced by the capsules is calculated first and used subsequently as a boundary condition for transmutation calculation.

In the first step a detailed model of the entire HFR core including experiments is used in an analysis with the Monte Carlo neutronic code MCNP4C3 [10]. In this analysis the flux in which the capsules are embedded is calculated in a 172 groups structure. These fluxes are used to calculate the fluence in the same four groups for which the fluence has been determined experimentally (see Table 3). The computed fluences deviate less than 10% from the experimental fluences, which is attributed to the uncertainty of the experimental results (5–10%) and the statistical error in the calculational results (1–5%). The result of this first step of the transmutation analysis is a flux in a fine group structure that is consistent with the available experimental data.

In the second step of the transmutation analysis the focus is on the change of the composition in the iodine capsules using a combination of MCNP4C3 and the burn-up code FISPACT [11]. A detailed model of the experiment is taken and embedded in the flux calculated in first step. The capsules that are also present in the model are divided into different zones and in each zone the flux is calculated using MCNP4C3. For each zone this flux and the composition of the zone is used as input for FISPACT, which then calculates the new inventory after a given time step. The inventories in the MCNP4C3 model are subsequently updated. After a sufficient number of time steps the entire irradiation

Table 3
Computed fluence and computed extent of transmutation

Capsule no.	Fluence (m^{-2}) in energy range				Total fluence	Extent of transmutation ($\Delta I/I$, %)
	1.353 MeV $< E <$ 19.6 MeV	67.3 keV $< E <$ 1.353 MeV	0.625 eV $< E <$ 67.3 keV	10^{-4} eV $< E <$ 0.625 eV		
6	3.42×10^{25}	6.12×10^{25}	8.87×10^{25}	3.35×10^{25}	2.18×10^{26}	3.55
7	3.23×10^{25}	5.79×10^{25}	8.79×10^{25}	3.25×10^{25}	2.11×10^{26}	3.70
8	3.10×10^{25}	5.55×10^{25}	8.34×10^{25}	3.24×10^{25}	2.02×10^{26}	3.79
9	3.17×10^{25}	5.68×10^{25}	8.25×10^{25}	3.32×10^{25}	2.04×10^{26}	3.85
10	3.39×10^{25}	6.07×10^{25}	8.66×10^{25}	3.32×10^{25}	2.14×10^{26}	3.80

history is simulated and the results of the transmutation analysis are obtained.

The results of the transmutation analysis are shown for each capsule in Table 3. These results show that the extent of the iodine transmutation varies from capsule to capsule in a way that is related to the iodine density. This suggest that (self)shielding is an important effect. This conclusion was checked by additional analysis in which the iodine density is reduced by a factor 10. For this reduced density the iodine transmutation is increased by almost a factor 2.

The influence of the nuclear data library was studied by replacing the JEF-2.2 library [12] with cross-sections based on JENDL-3.3 [13] and on recent measurements at JNC [14] in the thermal region. The use of these cross-sections increased the iodine transmutation by 0.1%, suggesting good agreement between both nuclear datasets.

The transmutation analyses have shown that the expected iodine transmutation varies between 3.55% and 3.80%. This variation is directly related to the iodine density and is due to the effect of neutron shielding by the samples. Variations of the nuclear data library have a small impact on these results.

5. Thermal behaviour

During irradiation the temperature of the aluminium drum surrounding the capsules is continuously monitored using thermocouples. The cycle-averaged temperatures of the five thermocouples placed in the vicinity of the five capsules were 365 °C. Small cycle-to-cycle temperature variations (about 15 °C) occur, due to changes in the loading of the HFR core.

In this experiment there is no generation of fission power and therefore all structural materials and the metal iodides were only heated by nuclear (gamma and neutron) heating. This causes the metal iodides to have a somewhat higher temperature than the cladding of the capsules. The melting temperatures of the presently irradiated metal iodides are relatively low (ranging from 595 °C for CuI to 783 °C for CaI_2). Therefore the temperature margin between the temperature of the cladding and the melting temperature of the metal iodide is relatively small. This is not only the case in the present irradiation, but this will be the case in probably any reactor concept to be used for LLFP transmutation. Parameters such as corrosion, vapour pressure and migration depend strongly on the temperature and on the fact if the metal iodide is solid or molten during irradiation.

The temperature distribution in the metal iodides is calculated using the following parameters: (i) the nuclear heating (ii) the temperature of the surrounding aluminium drum, (iii) the thermal conductivity of the metal iodides and the Xe–He gas (iv) the width of the gap surrounding the pellets. The accuracy of the temperature distribution computations is rather low due to large uncertainties in the thermal conductivity of the metal iodides and the thermal resistance of the gas gap surrounding the pellets. These two parameters will be discussed hereafter. Despite the above-mentioned large uncertainties the temperature distribution is assessed, since the temperature has a large influence on the in reactor behaviour of the metal iodides.

5.1. Thermal conductivity of the metal iodides

For the materials involved in the present irradiation only information could be found for NaI [15] and for CuI [16]. No thermal conductivity data could be found on MgI_2 and CaI_2. The thermal conductivity of NaI has been determined on solid material under external pressure. Extrapolated to zero pressure the thermal conductivity of NaI decrease from 3.9 W/m K at 120 K to 0.9 W/m K at 400 K. The thermal conductivity of CuI (density 5.63 g/cm^3) is 1.7 W/m K at 290 K. The thermal conductivity of metal iodides shows approximately an $1/T$ behaviour. The above-mentioned data only yields an indication on the thermal conductivity of the metal iodides in the present irradiation, due to:

- The influence of irradiation on the thermal conductivity of the fully dense metal iodides is unknown. In some materials irradiation causes for instance lat-

tice defects that reduce the thermal conductivity. The magnitude of this effect is strongly temperature dependent.

- The metal iodides in the present irradiation have a higher temperature than the temperature range in the literature data on thermal conductivity. This problem can partially be overcome using a $1/T$ extrapolation to 411 °C of the thermal conductivity, which yields a value of approximately 0.7 W/m K for CuI and 0.3 W/m K for NaI. The $1/T$ behaviour of the thermal conductivity is due to the temperature dependence of the phonon-scattering, influencing the phonon-contribution to the thermal conductivity. These extrapolated thermal conductivity values might be underestimations of the actual thermal conductivity, since for solid materials (amongst others oxides) a thermal conductivity of approximately 0.5–1 W/m K is the lower limit of the thermal conductivity [17].

5.2. Thermal resistance of the gas gap surrounding the pellets

The thermal resistance of the gas gap surrounding the pellets is influenced by the width of the gap and by the thermal conductivity of the gas in the gap. The width of the gap decreases during irradiation due to swelling of the metal iodide, causing the gap to be closed at the end of the irradiation. The xenon release during irradiation increases the xenon/helium ratio, decreasing the thermal conductivity of the gas. Table 4 shows that at the end of the irradiation the Xe:He ratio equals about 3.5:1 in all capsules. This reduces the thermal conductivity of the gas (793.2 K [16]) from 0.3 W/m K at BOI to 0.035 W/m K at EOI. The thermal resistance of the gap is decreased by the swelling of the metal iodides and increased by the xenon release. Whether the net effect of these two competing mechanisms is an increase or a decrease of the metal iodide temperature depends on the gas-release rate and the swelling rate over the irradiation period. Assuming a linear time dependence it can be estimated for the present cases that the metal iodide temperature slightly increases (about 10–30 degrees) during the first 100 irradiation days, after which the temperature step over the gap gradually decreases to zero due to the closure of the gap. Continuous pressure measurements during the irradiation of NaI pellets [8] suggest for that particular irradiation, that the gap between the pellets and the cladding is closed rather soon after the start of irradiation, while the xenon release from the pellets is low at the start of irradiation. This experimentally observed combination of gas-release and swelling will probably lead to a continuous temperature decrease of the metal iodide pellets during the first few irradiation cycles, after which the temperature stabilises for the remaining cycles.

5.3. Radial temperature profile

Using the finite element method the radial temperature profile has been computed for CuI and NaI at the start of irradiation (Fig. 3). These computations are based on the data shown in Table 5, the aluminium sample holder temperature of 365 °C and a nuclear heating of 8.0 W/g. It can be observed that the computed central temperatures are rather close to the melting temperature of both metal iodides. However, it should be kept in mind that the uncertainty in this computation is very large due to the uncertainty in the thermal conductivity of the metal iodides. The density of CuI (in g/cm^3) is higher than that of the other metal iodides in the present irradiation. Under the very course assumption that the thermal conductivities of all metal iodides are equal, CuI is expected to have a central temperature closest to its melting temperature, due to the relatively high density (and thereby high gamma heating) and its relatively low melting temperature. The temperature difference (ΔT) between the cladding temperature and the central temperature of the pellet varies between the metal iodides, mainly as a function of the density (ρ) of the metal iodide and the thermal conductivity (λ) of the metal iodide. The density of the metal iodide influences both the generated nuclear power (P) and the thermal conductivity of the metal iodide (λ), since this is influenced by the porosity. The proportionality is as follows:

Table 4
Gas puncturing results

Capsule no.	Compound	Plenum volume (ml)	Capsule pressure (bar SATP[a])	He (vol.%)	Xe (vol.%)	$^{128}Xe/I_{initial}$ molar ratio		
						Experimental	Computed	E/C
6	MgI_2	5.03	5.18	21.3	78.5	0.0390	0.0331	1.19
7	CaI_2		Capsule leak				0.0347	
8	CuI	5.00	4.86	20.8	78.7	0.0406	0.0348	1.17
9	NaI	5.00	4.24	24.7	75.0	0.0391	0.0360	1.08
10	NaI		Not measured				0.0351	

[a] Standard ambient temperature and pressure ($p = 0.1$ MPa, $T = 293.15$ K).

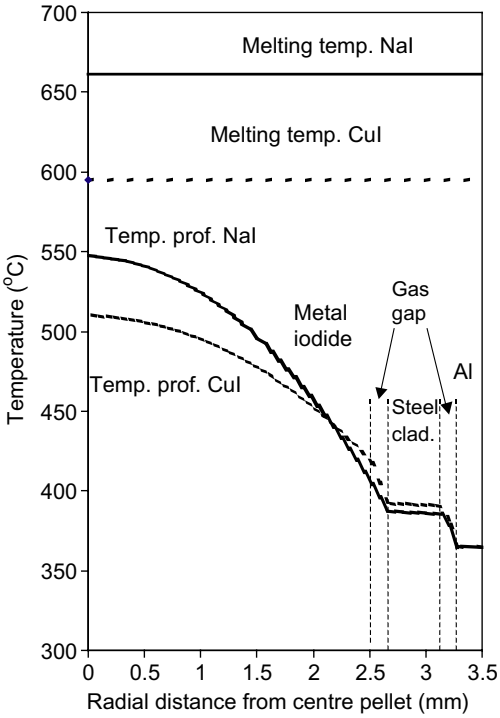

Fig. 3. Computed radial temperature profiles and the melting temperatures of NaI and CuI.

$$\Delta T \propto \frac{P}{\lambda} \propto \frac{\rho}{\lambda}, \tag{1}$$

where λ is calculated using the following equation that describes the influence of porosity on the thermal conductivity of a porous compound.

$$\lambda = \lambda_0 \times \left(\frac{\rho}{\rho_0}\right)^{3/2}, \tag{2}$$

ρ_0 and λ_0 are respectively the density and the thermal conductivity of 100% T.D. material. Eq. (2) is based on the assumption that the porosity is spherical and that the gas in the pores has a negligibly small thermal conductivity. The pores will mainly contain xenon gas which has a very low thermal conductivity compared to the metal iodides.

6. Post-irradiation examination

6.1. Neutrongraphs and X-ray images

Neutrongraphs and X-ray images were taken before and after irradiation in order to:

- Inspect the internals of the capsules and the sample holder before the start of irradiation.
- Study restructuring of the pellets after irradiation.
- Determine the dimensional changes of the pellet stacks.

The X-ray images (Fig. 2) and neutrongraphs made before irradiation show that all metal iodide pellets were properly positioned between the steel plugs and no anomalies were present. The neutrongraphs made after irradiation reveal that during irradiation no anomalies occurred, except for the steel plugs in the CuI capsule. The lengths of these plugs decreased with 0.9 mm due to corrosion. This finding is in agreement with the results of recent out-of-pile interaction tests between CuI and AISI316-stainless steel, in which chemical interaction was observed [3].

Comparing the X-ray images made before and after irradiation (e.g. Fig. 4) shows that the length of the metal iodides stack of all capsules has increased a few millimetres during irradiation. The relative dimensional changes are given in Table 6. Good consistency for the relatively length change of the two NaI capsules was found: 5.2% for capsule no. 9 and 5.5% for capsule no. 10. The smallest swelling of the metal iodide stack was found for CaI_2, then MgI_2 and NaI, and the largest stack swelling is found for CuI. On the X-ray images made after irradiation, the pellet–pellet interfaces and

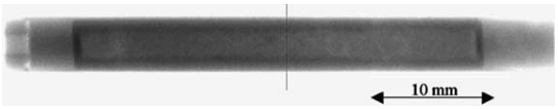

Fig. 4. X-ray image of capsule no. 8 (CuI) after irradiation in which a central region of lower density can be observed. The dotted line shows the position of the radial line scan, which is shown in Fig. 5.

Table 5
Data used for computation of the central temperature

Capsule no.	Sample	Initial gap width (mm)	Geometrical density (g/cm^3)	Thermal conductivity (W/m K)	Computed pellet central temperature (°C)	Melting temperature (°C)
8	CuI	0.152	5.04	0.7	510	595
9/10	NaI	0.154	3.39	0.3	547	661

Table 6
Data obtained from analysis of the X-ray images before and after irradiation

Capsule no.	Sample	Relative change (%)		
		Pellet stack length	Pellet diameter	Pellet stack volume
6	MgI_2	4.1	6.0	17.0
7	CaI_2	1.7	5.9	14.0
8	CuI	12.5	6.0	26.5
9	NaI	5.2	6.1	18.5
10	NaI + PT	5.5	6.1	18.8

pellet–cladding interfaces were no longer visible, showing strong swelling and gap closure during irradiation.

Radial line scans of the X-ray images before and after irradiation have been made (Fig. 5). The line scans made before irradiation (BOI) show the cladding and the gap between the pellets and the cladding. After irradiation the gap is closed in all capsules, which corresponds to a radial swelling of the pellets of about 6%. Combining the radial and the axial swelling yields a volume swelling of 14.0–26.5%. The swelling is probably induced by the combined effect of: (i) transport of metal iodide from hotter to colder regions, (ii) the xenon production in the pellets. Note that the volume swelling found (14%–26.5%) during the cause of the irradiation is larger than the thermal expansion (6.4–11%, Table 1). From the present results it is difficult to say if there is any relation between the volume swelling and the thermal expansion.

The X-ray images at EOI show a dip in the optical density in the centre of some of the fuel stacks. This dip is most pronounced in CuI and MgI_2, less pronounced in NaI and absent in CaI_2. Analysis of the line scans suggests that a low-density central column is formed. The estimated density of the central region of CuI is roughly 50–75% of that of the outer region of the CuI pellets. The formation of the less dense central region is most clearly observed in CuI (approximate width 3 mm), which might be attributed to the relatively high vapour pressure of CuI.

The X-ray images made after irradiation show almost no axial variations, in the metal iodide densities along the height of the metal iodide stacks. The combination of the absence of an axial profile in the metal iodide density and the axial elongation of the metal iodide stacks strongly suggest that in none of the capsules melting has occurred.

6.2. Gas puncturing and gas analysis

The capsules were punctured and the gas composition (including isotopic composition) was analysed (Table 4). Based on these results the measured molar ratio $^{128}Xe/I_{initial}$ is shown in Table 4 together with the

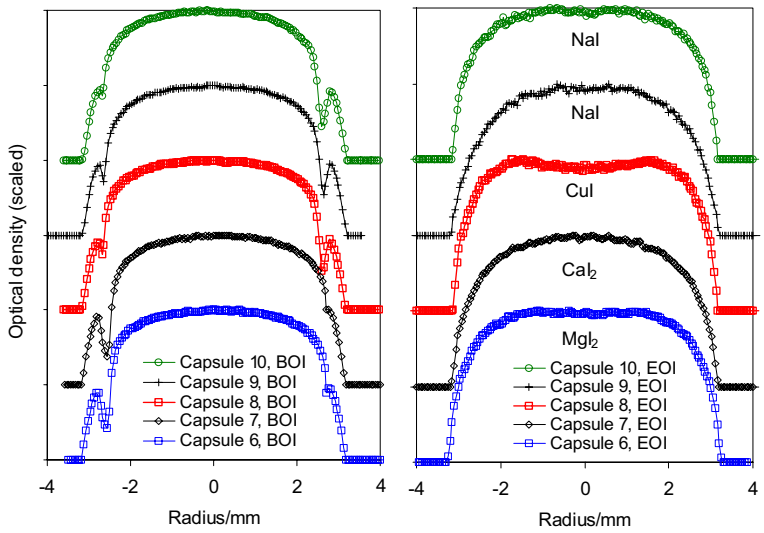

Fig. 5. Radial line scans of the optical density of X-ray images taken at the beginning of irradiation (BOI) and the end of irradiation (EOI). The blackening of the film is plotted as a function of the radial position.

computed amount using the neutronics method described in Section 4.

For capsule no. 7 a low capsule pressure of 0.49 bar was found, which can only be explained by a leak in the capsule disturbing the puncturing procedure. Capsule no. 10 has not been punctured. The measured helium concentration and capsule pressure are in good agreement with the He-gas pressure slightly over 1 bar present at the start of irradiation. Comparing the measured $^{128}Xe/I_{initial}$ ratio with the MCNP calculated $^{128}Xe/I_{initial}$ ratio shows good agreement. The observed slightly higher measured value (8–19% higher) for the $^{128}Xe/I_{initial}$ ratio is partially induced by the fact that the MCNP model used the BOI dimensions of the metal iodide pellets. Due to the swelling during irradiation (Table 6) the density of the pellet stacks decreased and the volume increased. From the strong neutron self-shielding discussed in Section 4 it can be concluded that an increase in volume will increase the transmutation significantly. Repeating the MCNP computation for CuI using the dimensions and density of the CuI pellet stack after irradiation (Table 6) gave a 3.5% higher value for the $^{128}Xe/I_{initial}$ ratio compared to the BOI computation. Effects that may further be of influence on the difference between the measured and computed ratio are either:

- MCNP computes the amount of ^{128}Xe produced, whereas the amount of ^{128}Xe released is measured. However, assuming that some of the ^{128}Xe produced is not released, would lead to a larger difference between the measured and computed ratio.
- Inaccuracy in the experimental conditions (e.g. variations in the flux level and spectrum) and inaccuracies in the analytical techniques (e.g. puncturing and gas analysis).
- Inaccuracy in the nuclear computations, such as inaccuracy of the nuclear data and in the computational method used.

The fact that good agreement is found between the experimental and the computational $^{128}Xe/I_{initial}$ ratio suggests that complete xenon release from all the metal iodides took place during the irradiation. The project-I PSF experiment [8] in which the temperature dependence of the xenon release from NaI is studied showed that the release is fast at temperatures close to the melting point. Since the present thermal computations showed that the temperatures of NaI and CuI are close to the melting temperature, it is to be expected that for the present experiment complete xenon release will take place, which is in agreement with the measured data. It can be computed using Eq. (3), the measured $^{128}Xe/I_{initial}$ ratio and the information on the ^{128}Te, ^{129}Xe and ^{130}Xe formation that the iodine transmutation extent ($\Delta I/I$) in the present experiment ranges are 4.18% (MgI_2), 4.36% (CuI) and 4.20 (NaI). F.G.R. in Eq. (3) marks the fractional gas release, which is assumed to be 1 for the present case and the number 0.94, which corrects for the formation of tellurium.

$$\frac{\Delta I}{I} = \frac{(^{128}Xe/I_{initial})}{0.94F.G.R}. \quad (3)$$

6.3. Chemical analysis and gamma spectrometry

After gas puncturing the capsules were opened using a cutting device. The pellets were stuck to the cladding, which is in agreement with the X-ray images made after irradiation. The irradiated metal iodides were recovered by rinsing with distilled water containing a small amount of NH_4OH (pH = 8), in order to lower the vapour pressure of HI and I_2. In the case of CuI an alkaline solution containing a high concentration of NH_4OH was used to improve the solubility of CuI. Visual inspection of the rinsed water showed black precipitates in some of these samples, which presumably originate from corrosion of the cladding. These solutions were prepared for chemical analysis and gamma spectrometric analysis in order to:

- Determine the presence of corrosion products from the cladding. The dose rate of the solutions was measured after which it became clear that sample no. 8 (CuI) shows a very high dose rate (approximately 500 μSv/h at 10 cm), indicating a strong corrosive effect of this sample. Gamma-spectrometry on various isotopes has been performed. Using the ^{60}Co activity in the solution as an indicator for corrosion progress, MgI_2 shows a somewhat stronger corrosion than CaI_2 and NaI, which corresponds with the results of the pre-irradiation compatibility test.
- Determine the metal/iodine ratio after irradiation and compare these data with the data on the unirradiated starting material. In principle, this yields information on the extent of iodine transmutation. Titration and neutron activation analysis were used to assess the absolute amounts of iodine and metal. No consistent results for the iodine to metal ratio could be obtained. This was due to the fact that complete recovery of all metal and iodine from the capsules could not be obtained, which made it impossible to accurately determine the I-transmutation in this way.

6.4. Metallography

After the capsules were rinsed with water, parts of the capsule were cut for metallographic inspection. These pieces were taken from the axial position where the pellet stack was located. No damage or severe cladding corrosion could be found on these images. Except for

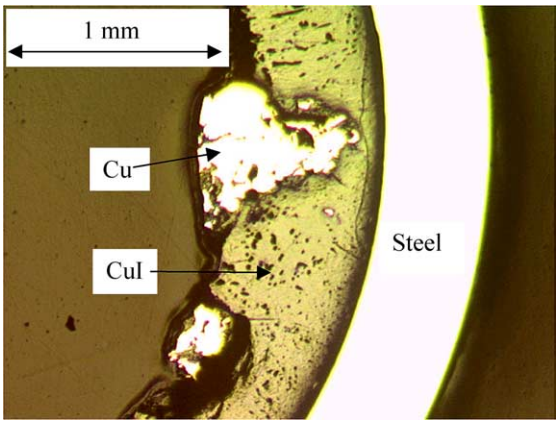

Fig. 6. Metallographic detail of capsule no. 8 (CuI).

CuI no remains of the salts were observed in these metallographies. This is in agreement with the fact that CuI is the only presently studied metal iodide that does not dissolve in water. The remainder of copper iodide has an annular shape (Fig. 6). This annulus is interesting because the X-ray inspection after irradiation (Figs. 4 and 5) shows an annular higher density CuI region. The connection between these two annular phenomena is not exactly clear. Another interesting feature of the CuI is the fact that pieces of metallic Cu were found (Fig. 6) which can be described by the following overall reaction:

$$\mathrm{CuI} \rightarrow \mathrm{CuI}_{1-y} + y\mathrm{Xe} \rightarrow y\mathrm{Cu} + \mathrm{CuI} + y\mathrm{Xe}.$$

This may be due to evaporation of iodine. According to Shirasu and Minato [3] CuI evaporates incongruently and I_2 and I are the main gaseous species above CuI. The iodine gas can chemically interact with steel, enhancing the copper particle formation. The combination of differences in the partial pressure of the various compounds and the radial temperature profile may further enhance the copper particle formation. The above-mentioned copper particle formation might also be enhanced by the reduction of the iodine concentration due to transmutation.

Electron probe micro-analysis measurements have been done on the region shown in Fig. 6. These measurements confirmed that the metallic inclusion is indeed copper and the other phase is CuI with a copper to iodine ratio close to 1.

6.5. Discussion and conclusions

The project-I research programme was performed successfully. The programme comprised the fabrication, irradiation and post-irradiation examinations of four metal iodides: NaI, CuI, MgI_2 and CaI_2. Pellets of metal iodide powders were prepared and loaded in capsules. The capsules were irradiated for 271.23 full power days in the High Flux Reactor. The main parameters for the studied metal iodides are shown in Table 7. On the basis of project-I results none of these metal iodides can be disqualified, although the corrosion problem of CuI may have to be overcome by optimisation of the cladding. Making a choice between the metal iodides will depend strongly on the scenario, which might be used for large-scale iodine transmutation. In general, the iodine transmutation target should fulfil requirements of fabrication, irradiation, recycling (target dissolution and re-fabrication). Given the rather slow transmutation rate of iodine-129, recycling of the iodine targets is presumably inevitable. Concluding one can say that CaI_2 performs well under irradiation conditions, it has a limited swelling and does not from a low-density region in the centre of the stack. It has the highest melting point and lowest vapour pressure of the tested samples, but it has the drawback that it is very sensitive to air. CuI is insoluble in water and stable in air, but shows strong corrosion with the cladding material under irradiation conditions. CuI, NaI and MgI_2 have comparable melting points, but NaI is the only compound of which the metal (Na) has a melting point lower than the irradiation temperature. CuI, NaI and MgI_2 released nearly all xenon formed under the current irradiation conditions. NaI and MgI_2 have mediocre properties in many aspects, but especially the ease of handling of NaI, caused by its relatively good stability in air, is beneficial. Shirasu and Minato [3] studied the properties of MgI_2, CaI_2, CuI, $Ca(IO_3)_2$ and NaI and performed out-of-reactor heating experiments of CuI and $Ca(IO_3)_2$ with various cladding materials. The main conclusion is that CuI has the large advantage that it is stable to air and the disadvantage that it reacts with a stainless steel

Table 7
The main results for the studied metal iodides

	CaI_2	NaI	MgI_2	CuI
Chemical compatibility with 316L steel[a]	+	+	±	–
Volume change (%)	14.0	18.7	17.0	26.5
Formation of less dense region	Not observed	Yes	Yes	Yes

[a] Results from cladding/salt compatibility experiments.

cladding. Using a copper-liner at the inside of the cladding might prevent the corrosion of the cladding.

References

[1] R.J.M. Konings, J. Nucl. Mater. 244 (1997) 16.
[2] E. Ichimura, Iodine selection criteria results, unpublished.
[3] Y. Shirasu, K. Minato, J. Nucl. Mater. 320 (2003) 25.
[4] Gardner, BMRI 7040, reported by the International Centre for Diffraction Data (JCPDS) 2003.
[5] L.V. Gurvich, I.V. Veyts, C.B. Alcock, in: Thermodynamic Properties of Individual Substances, vol. III, CRC Press, New York, 1994.
[6] I. Barin, Thermochemical Data of Pure Substances, VCH, 1994.
[7] D.A. Keen, S. Hull, J. Phys.: Condens. Matter 7 (1995) 5793.
[8] R.P.C. Schram, K. Bakker, R. Klein Meulekamp, E. Ichimura, N. Takaki, Results of the Proj-I-PSF irradiation, unpublished.
[9] L.H. Baetsle (chairman of experts group), Actinide and fission product partitioning and transmutation, Report of the Nuclear Energy Agency, 1999.
[10] J.F. Briesmeister (Ed.), LA-13709-M, Los Alamos report, USA, 2000.
[11] R.A. Forrest, J.-Ch. Sublet, UKAEA FUS 287, UKAEA Government Division Fusion Report, Oxfordshire, 1995.
[12] JEFF Report 17, OECD Nuclear Agency, Paris, France, 2000.
[13] K. Shibata, T. Kawano, T. Nakagawa, O. Iwamoto, J. Katakura, T. Fukahori, S. Chiba, A. Hasegawa, T. Murata, H. Matsunobu, T. Ohsawa, Y. Nakajima, T. Yoshida, A. Zukeran, M. Kawai, M. Baba, M. Ishikawa, T. Asami, T. Watanabe, Y. Watanabe, M. Igashira, N. Yamamuro, H. Kitazawa, N. Yamano, H. Takano, Japanese Evaluated Nuclear Data Library Version 3 Revision-3: JENDL-3.3, J. Nucl. Sci. Technol. 39 (2002) 1125.
[14] T. Katoh, S. Nakamura, H. Harada, Y. Ogata, J. Nucl. Sci. Technol. 36 (1995) 223.
[15] B. Hakansson, P. Andersson, J. Phys. Chem. Solids 47 (1986) 355.
[16] Y.S. Touloukian, P.E. Liley, S.C. Saxena, in: Thermophysical Properties of Matter, vol. 3, IFI/Plenum, New York, 1970.
[17] G.A. Slack, in: Solid State Physics: Advances in Research and Applications, vol. 34, Academic Press, New York, 1979.